Hindawi Publishing Corporation
Journal of Chemistry
Volume 2015, Article ID 959012, 9 pages
http://dx.doi.org/10.1155/2015/959012

Research Article

Removal of Chlorinated Chemicals in H_2 Feedstock Using Modified Activated Carbon

Prapaporn Luekittisup,[1,2] Visanu Tanboonchauy,[3] Jitlada Chumee,[4] Somrudee Predapitakkun,[5] Rattanawan W. Kiatkomol,[5] and Nurak Grisdanurak[6,7]

[1]*International Program in Hazardous Substance and Environmental Management, Graduate School, Chulalongkorn University, Bangkok 10300, Thailand*
[2]*Center of Excellence on Hazardous Substance Management (HSM), Chulalongkorn University, Bangkok 10300, Thailand*
[3]*Department of Environmental Engineering, Faculty of Engineering, Khon Kaen University, Khon Kaen 40002, Thailand*
[4]*Department of Chemistry, Faculty of Science and Technology, Suan Sunandha Rajabhat University, Bangkok 10300, Thailand*
[5]*PTT Research and Technology Institute, Wong Noi, Ayutthaya 13170, Thailand*
[6]*Center of Excellence in Environmental Catalysis and Adsorption, Thammasat University, Pathumthani 12121, Thailand*
[7]*Department of Chemical Engineering, Faculty of Engineering, Thammasat University, Pathumthani 12121, Thailand*

Correspondence should be addressed to Nurak Grisdanurak; gnurak@engr.tu.ac.th

Received 2 March 2015; Revised 9 June 2015; Accepted 17 June 2015

Academic Editor: Maria N. D. S. Cordeiro

Activated carbon (GAC) was impregnated by sodium and used as adsorbent to remove chlorinated hydrocarbon (CHC) gases contaminated in H_2 feedstock. The adsorption was carried out in a continuous packed-bed column under the weight hourly space velocity range of 0.8–1.0 hr^{-1}. The adsorption capacity was evaluated via the breakthrough curves. This modified GAC potentially adsorbed HCl and VCM of 0.0681 $g_{HCl}/g_{adsorbent}$ and 0.0026 $g_{VCM}/g_{adsorbent}$, respectively. It showed higher adsorption capacity than SiO_2 and Al_2O_3 balls for both organic and inorganic CHCs removal. In addition, the kinetic adsorption of chlorinated hydrocarbons on modified GAC fit well with Yoon-Nelson model.

1. Introduction

Natural gas received directly from wells contains a variety of hydrocarbons. Dienes are one of the active hydrocarbons. They readily react with chloride compounds to form chlorinated hydrocarbons under severe conditions [1]. Chlorinated hydrocarbons can be generated in both organic and inorganic forms and can contaminate downstream feedstocks. It possibly causes the corrosion in pipelines and the catalyst poisoning and so forth. Twigg and coworker (2003) [2] revealed that the activity of $Cu/ZnO/Al_2O_3$ on water gas shift reaction was reduced from 100 to 60% within an hour time on stream when the H_2 was contaminated with an extremely low concentration of chlorinated hydrocarbons ca. 0.03 vol%. It is therefore necessary to eliminate chlorinated hydrocarbons from the feedstocks. According to their low contaminated concentration, removal by adsorption could be a promising technique. However, it might be difficult to include all CHCs in the study. Hydrogen chloride gas (HCl) and vinyl chloride gas (VCM) were used as probe representatives of inorganic CHCs and organic CHCs, respectively, for the study.

A chloride guard bed is applied industrially to remove the Cl species from the H_2 feedstock. The chloride guard bed works basically on the adsorption principle. Commercial adsorbents used in this treatment are zeolite based and are effective for inorganic CHCs.

Activated carbon is a general adsorbent that is used in technologies related to pollution treatment due to its highly porous, surface area, and large adsorption capacity. It has been reported that activated carbon is effectively applied to any organic vapor substance removal [3–5]. The adsorption ability of activated carbon depends on the functional groups cooperated on its surface, surface area, and pore structure. Normally, the functional groups on activated carbon are

associated with high concentration of unpaired electrons in imperfect sections of graphite that can react with molecular oxygen to form carbon-oxygen surface complexes such as carboxyl, lactone, phenol, carbonyl, ether, pyrone, and chromene. These surface groups present an acid-base character of activated carbon that can adsorb organic compounds [6, 7]. To improve the inorganic gas adsorption onto activated carbon, it should be modified by adding a positive charge of the metal on surface such as by electroplating or soaking with metal solution to enhance the adsorption efficiency [8].

The Ag and Ni nanoparticles were electroplated on the surface of activated carbons fibers (ACFs). When HCl was adsorbed on the surface, it formed AgCl and $NiCl_2$ more effective for HCl removal than untreated ACFs [9–11]. Nevertheless electroplating and transition metals are high-cost operations. Consequently, alkaline metal, like Na, has been considered due to cheap and nontoxic. A few studies of HCl adsorption by active carbon modified Na have been done. The tests were carried out in HCl concentration of about 1,000 ppm under humid condition. Activated carbon modified Na showed an effective performance and was reused repeatedly [8]. However, the removal of VCM through adsorption has not been publicly reported.

The goal of this work was to prepare modified activated carbon by chemical treatment methods for both HCl and VCM removal in a continuous fixed bed flow reactor. The work focused on the removal of low concentration of contaminating gases. The physicochemical properties were also analyzed to support the adsorption phenomena. Also, suitable kinetic models, Thomas model and Yoon-Nelson model, were applied to examine the reaction pathways and mechanism of adsorption process.

2. Materials and Methods

2.1. Materials. Alumina balls and silica were purchased from Pingxiang Huihua Packing Co., Ltd., China. Mixed gases of HCl in H_2 and VCM in H_2 were prepared and provided by TIG (Thailand Industrial Gas Co., Ltd., Thailand).

2.2. Preparation of Modified Activated Carbon. Activated carbon used in this work was in granular form, GAC, supported by Carbokarn Co., Ltd., Thailand. The properties of GAC are presented in Table 1. Particle size of as-received GAC 8×16 in the study was in the average size of US standard sieve mesh size of 2.36–1.18 mm. The modified activated carbon was prepared by soaking 12 g GAC in 6 N and 12 N solution for 3 h. Afterwards, it was filtered and dried at 80°C overnight. The obtained material was denoted as NaOH/GAC. Sodium content of the NaOH/GAC was determined using a titration technique.

3. Experiment

3.1. Adsorption Studies of VCM and HCl. Adsorption performances of studied adsorbents were carried out in a continuous packed-bed column. The column of 1 cm diameter was constructed with glass. Approximately 1 g of studied adsorbent was packed in 3 layers alternated with quartz wool. Each layer was packed 2 cm high. Feed gas with major component of H_2 contaminated with either 600 ppm HCl or 20 ppm VCM was fed into the column at a rate of 50 mL/min as shown in Figure 1. Effluent from the adsorption column was measured using special gas detector tube numbers 14L-14M and 131La for HCl and VCM, respectively. Detection limits for each gas detector tube are 0.05 ppm. All adsorbents for HCl and VCM removal were compared with commercial SiO_2 and Al_2O_3 balls.

Table 1: Typical properties of GAC from Carbokarn Co., Ltd., Thailand.

Source	Coconut shell	
Iodine number (mg/g)	1254	
CTC adsorption (%)	57.2	
Particle size distribution	+8	7.4
	8×16	90
	−16	2.6
Moisture content (%)	5.3	
Corrected bulk density (g/mL)	0.5	

Table 2: BET-surface area of all adsorbents.

Adsorbent	Surface area (m^2/g)
SiO_2	85
Al_2O_3 ball	307
GAC	995
6 N NaOH/GAC	846
12 N NaOH/GAC	258

3.2. Characterization of Adsorbents. Both fresh and spent adsorbents were characterized for their physicochemical properties by BET-surface area (Autosorb-1 Quantachrome, BL model), X-ray diffraction (XRD; BRUKER AXS: D8 ADVANCE A25), scanning electron microscopy (SEM; Jeol scanning microscope model JSM-5410), X-ray fluorescence (XRF; Philips PW 2400), and Fourier transform infrared spectrometer (FTIR; BRUKER TENSOR27).

4. Results and Discussion

4.1. Characterization. BET-surface area of all adsorbents is presented in Table 2. SiO_2 and Al_2O_3 balls were used as references. GAC possessed higher surface area compared with other adsorbents. Considering the modification of GAC with Na in different loadings, it was obvious that the more the Na loading is, the lower the surface area of modified GAC was observed. Surface area of 12 N NaOH/GAC was lower by four-five times compared to 6 N NaOH/GAC and fresh GAC, respectively. This might be due to Na flakes, which were crystallized out during the preparation, covered, and blocked micro- and mesopores of GAC, as will be discussed in the following.

Even though the higher Na content may benefit the HCl adsorption capacity, it might not be good for VCM removal,

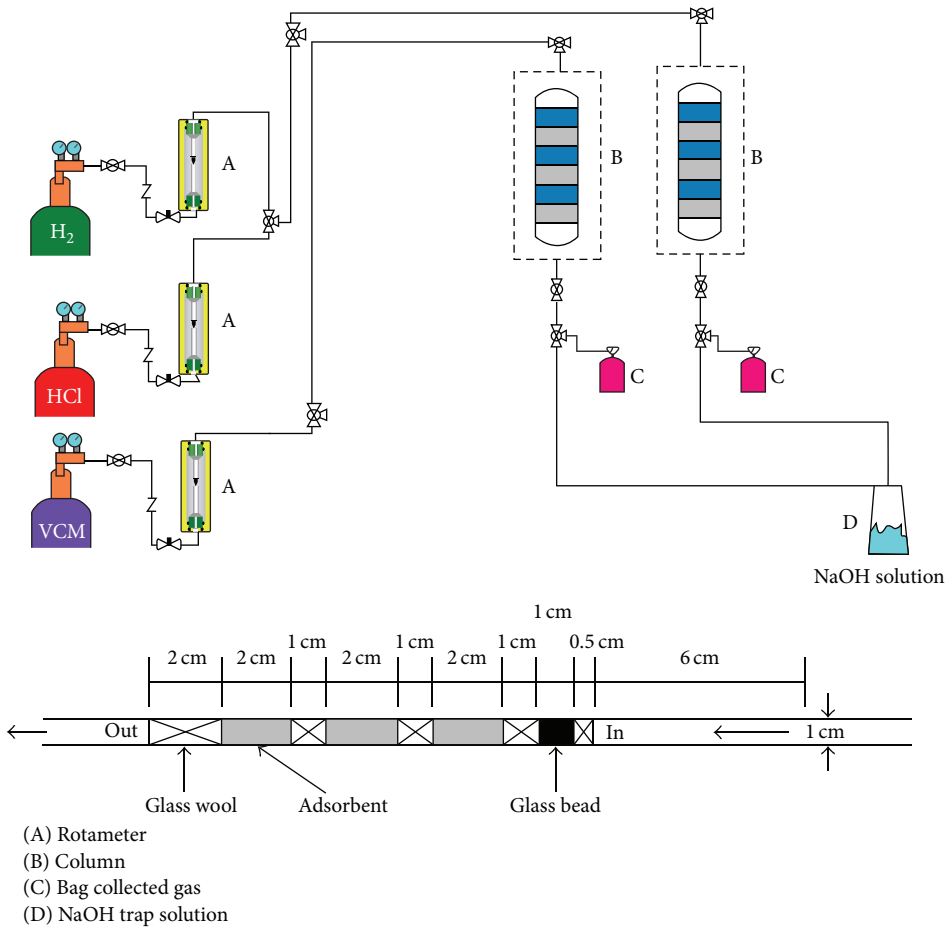

Figure 1: Fixed-bed flow column.

because of low surface area. To optimize the adsorption for both chloride species, 6 N NaOH/GAC was selected for further study.

The surface property of 6 N NaOH/GAC is confirmed by N_2 adsorption-desorption measurement, shown in Figure 2. Modified GAC with Na still had the isotherm of type I according to the IUPAC classification, similar to that of GAC. The only observation was that the adsorbed amount of NaOH/GAC was lower than GAC indicating that its surface area decreased after NaOH addition, as described in Table 2. This suggested that sodium at this concentration had not affected GAC physical structure.

SEM images of GAC and NaOH/GAC are shown in Figure 3. The structure and morphological characteristics of microcrystalline cellulose and lignin were observed [12, 13]. The external surfaces of GAC presented smooth open pores of different sizes. The large pores in GAC contained multiple smaller pores like sponge as shown in cross section image (Figure 3(b)). Most micropores with nearly uniform dimensions were observed. On the other hand, the external surfaces of NaOH/GAC presented disappearance of microcrystalline cellulose and pore blocking due to the flakes of Na crystals. This was also seen in the cross-sectional images, corresponding with the decrease of BET-surface area results.

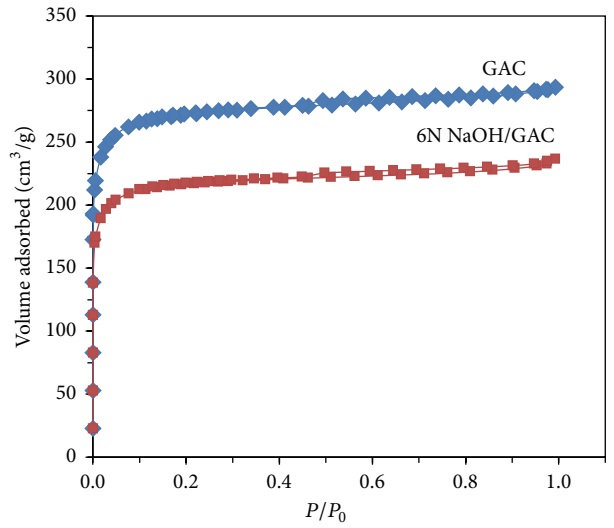

Figure 2: N_2 adsorption-desorption isotherm of GAC and NaOH/GAC.

The structures of GAC, 6 N NaOH/GAC (both fresh and spent), were confirmed by FT-IR spectrum. According to Figure 4, all materials show the FT-IR spectra at 3435 cm^{-1}

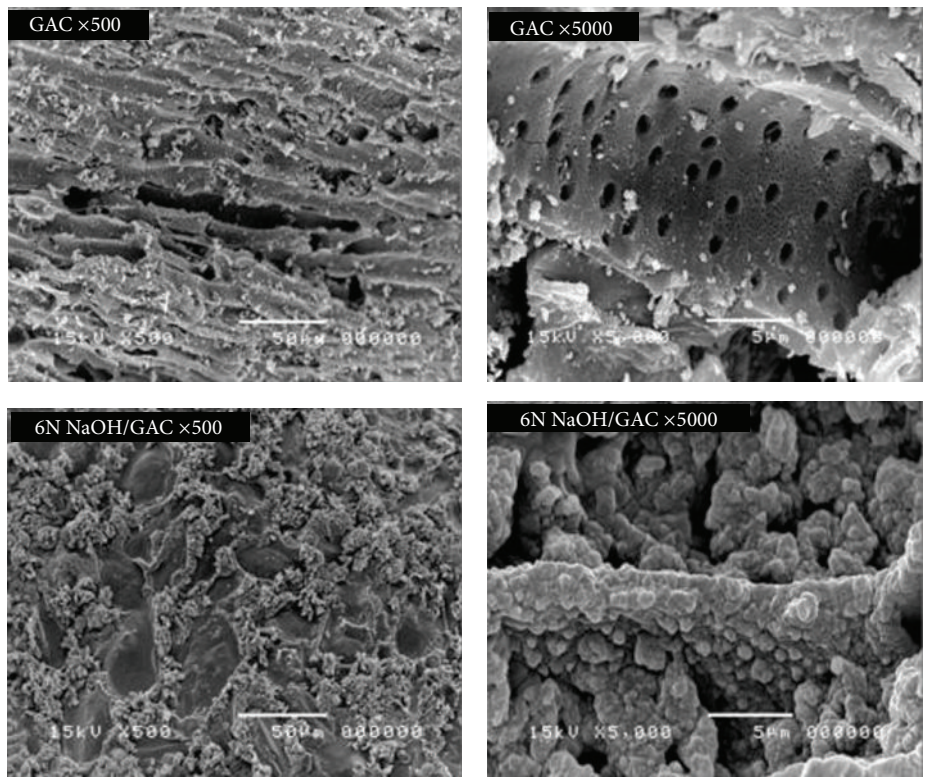

Figure 3: SEM images of GAC and NaOH/GAC; (a) external surface and (b) cross-sectional surface.

indicating O–H stretching vibration mode of OH^- groups or adsorbed water, while the band at 2930 is attributed to C–H interaction with the surface of the carbon. The bands around 1096 cm^{-1} are confirmed to pertain to ring vibration in a large aromatic skeleton generally found in carbonaceous material. Considering the spectra of 6 N NaOH/GAC, The bands between 1384 and 1450 cm^{-1} are observed, assigned to –OH bending vibration that present strong peak when NaOH was added [14]. After the adsorption of HCl, the intensity of this band was decreased, while the adsorbed water peak became boarded. This might be due to higher available NaCl.

4.2. HCl and VCM Adsorption. 6 N NaOH/GAC is selected to study for the dynamic HCl and VCM adsorption tests as shown in Figures 5(a) and 5(b), respectively. The performance of 6 N NaOH/GAC was presented in breakthrough curves against those of GAC, SiO_2, and Al_2O_3 ball.

HCl Performance. The adsorption of HCl shows a sudden breakthrough (Figure 5(a)), indicating that the adsorption phenomenon relies on the amount of functional metal on the surface of the adsorbent. SiO_2, which was metal-free, was ineffective to HCl, while GAC with the Na loading illustrated the highest adsorption.

Areas above the breakthrough curves were evaluated for bed adsorption capacity (W_b) and saturated adsorption capacity (W_s) as well as bed capacity. W_b is the dynamic adsorption capacity considered within the mass transfer zone

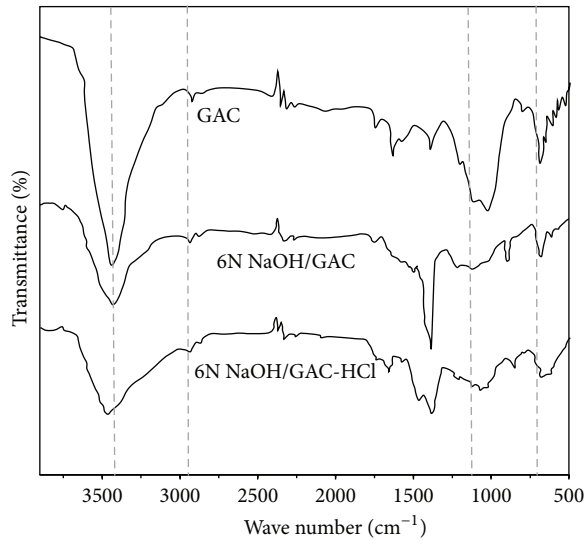

Figure 4: FTIR spectrum of GAC and modified GAC.

($C/C_0 < 0.05$), whereas W_s covers the entire adsorption capacity (both mass transfer zone and saturated zone). The calculated results are tabulated in Table 3. In practical work, value of W_b is seriously considered. Considering W_b, the adsorption potential of HCl over 6 N NaOH/GAC exhibited 0.0681 g_{HCl}/g, which was about twice than that on GAC

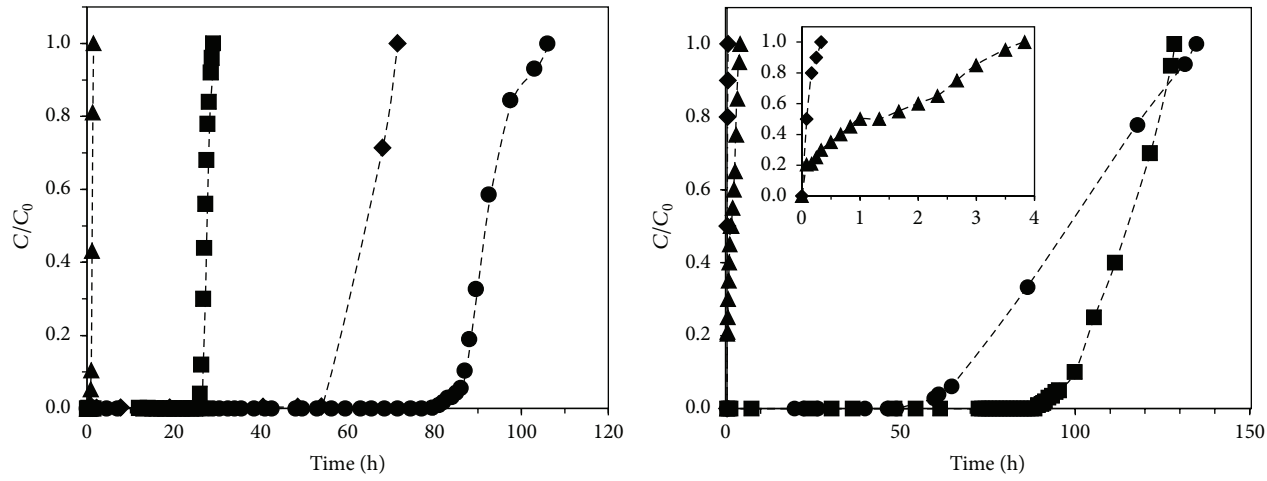

Figure 5: Breakthrough curves of HCl (int. 600 ppm) and VCM (int. 20 ppm) contaminated in H_2; ■ GAC, ● 6 N NaOH/GAC, ▲ SiO_2, and ▼ Al_2O_3 balls.

Table 3: HCl and VCM adsorption capacity over adsorbents.

Adsorbent	HCl			VCM		
	W_b (g_{HCl}/g)	W_s (g_{HCl}/g)	Bed capacity	W_b (g_{VCM}/g)	W_s (g_{VCM}/g)	Bed capacity
GAC	0.0259	0.0275	0.9467	0.0063	0.0078	0.8134
6 N NaOH/GAC	0.0681	0.0627	0.9364	0.0026	0.0041	0.6504
SiO_2	0.0011	0.0015	0.7246	1.57×10^{-6}	1.27×10^{-4}	0.0123
Al_2O_3 ball	0.0301	0.0356	0.8448	2.28×10^{-7}	4.01×10^{-6}	0.0569

(0.0259 g_{HCl}/g) and higher than those on SiO_2 and Al_2O_3. The bed capacities of each adsorbent, except for SiO_2, were close to perfect. This indicated that the adsorbent was packed uniformly without a channeling effect.

VCM Performance. The adsorption of VCM shows both sudden breakthrough and gradual breakthrough (Figure 5(b)), indicating that the adsorption phenomena relied on availability of surface area of adsorbent. SiO_2, which had very low surface area (85 m^2/g), accepted very little uptake of VCM (W_b = 1.57×10^{-6} g_{VCM}/g) and reached the breakthrough within 30 min. On the other hand, GAC and 6 N NaOH/GAC, which had higher surface areas (840–900 m^2/g), showed comparatively high adsorption capacity (W_b = 0.0026 g_{VCM}/g). This indicated that surface area played a key role for organic CHCs adsorption. In addition, bad packing may have caused channeling effect in GAC and 6 N NaOH/GAC tests. Smaller particle size was therefore recommended for the further test.

It was interesting to investigate the reduction of HCl and VCM in the adsorption process. Since low concentration of VCM (20 ppm initially) was used for the study, the diagnosis of the adsorbent surface would be difficult. Therefore, only samples of spent adsorbents from all layers of the HCl guard were characterized by XRD and XRF. Figure 6 illustrates XRD patterns for GAC (Figure 6(a)) and 6 N NaOH/GAC (Figure 6(b)) on each layer, respectively.

XRD pattern of GAC (Figure 6(a), top spectrum) shows two broad peaks around 23° and 43°, which could be attributed to the presence of carbon and graphite [14]. After loading NaOH, the XRD pattern of 6 N NaOH/GAC (Figure 6(b), below spectrum) showed sharp peaks at 30° and small peaks around 32–50° corresponding to crystalline of NaOH deposited on granular activated carbon surface.

Considering Figure 6(a) for the spent adsorbents, there was an insignificant change of XRD pattern compared to fresh GAC. This was confirmed that chemisorption of HCl on GAC did not take place during the adsorption. On the other hand, XRD patterns of 6 N NaOH/GAC from each layer differed from the original one. It was expected that sodium content in GAC structure reacted with HCl to form salt (NaCl) crystalline. To confirm the deposition of NaCl onto the adsorbent, the XRD pattern of NaCl crystal attached is identical to the patterns in spent material, as shown in Figure 6(b), top spectrum.

Table 4 lists the content of Cl element remaining in each adsorbent layer, characterized by XRF. As seen, the amount of Cl residue is high compared to an initial Cl content. This confirmed the successful improvement of inorganic CHCs removal by the modified GAC with Na loading.

4.3. Kinetic Approach. In order to apply our adsorption results to the practical use, the adsorption kinetics should

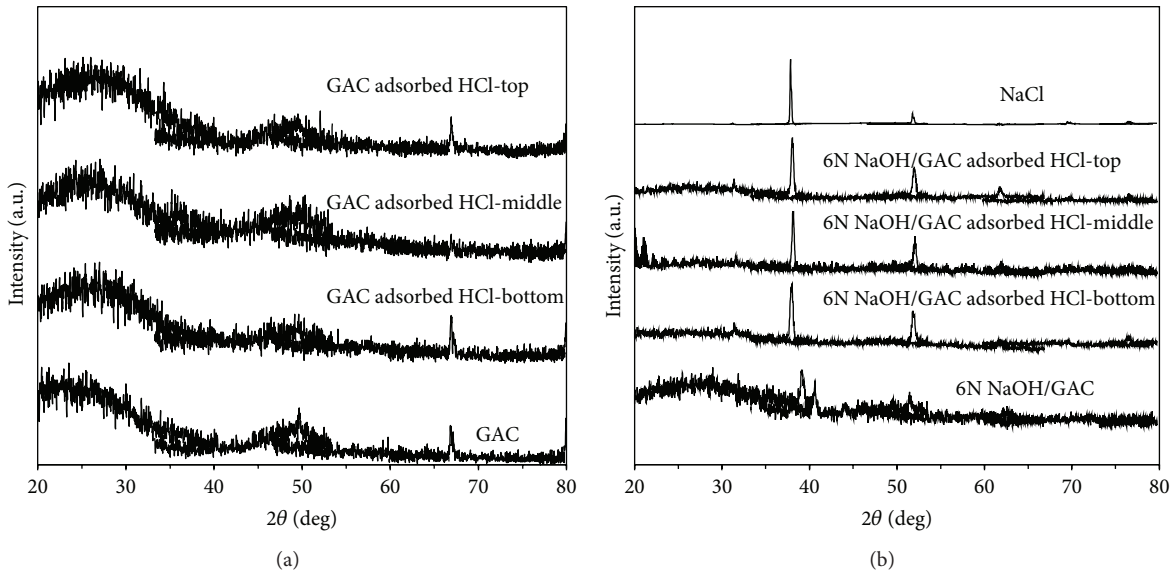

Figure 6: XRD patterns of GAC and 6 N NaOH/GAC after HCl adsorption.

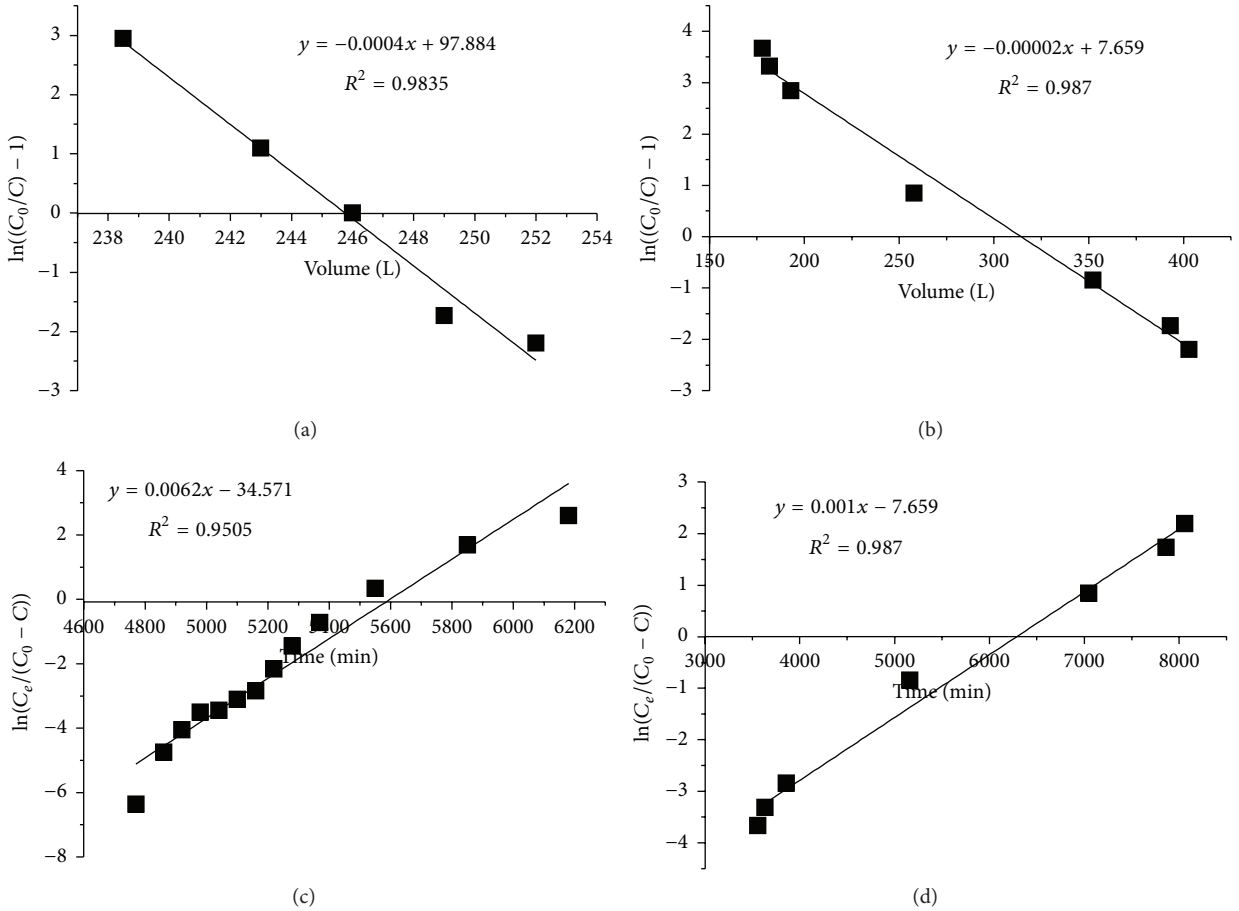

Figure 7: Plots of linearized kinetic approach results for the adsorption of (a) HCl and (b) VCM using Thomas model; (c) HCl and (d) VCM using Yoon-Nelson model.

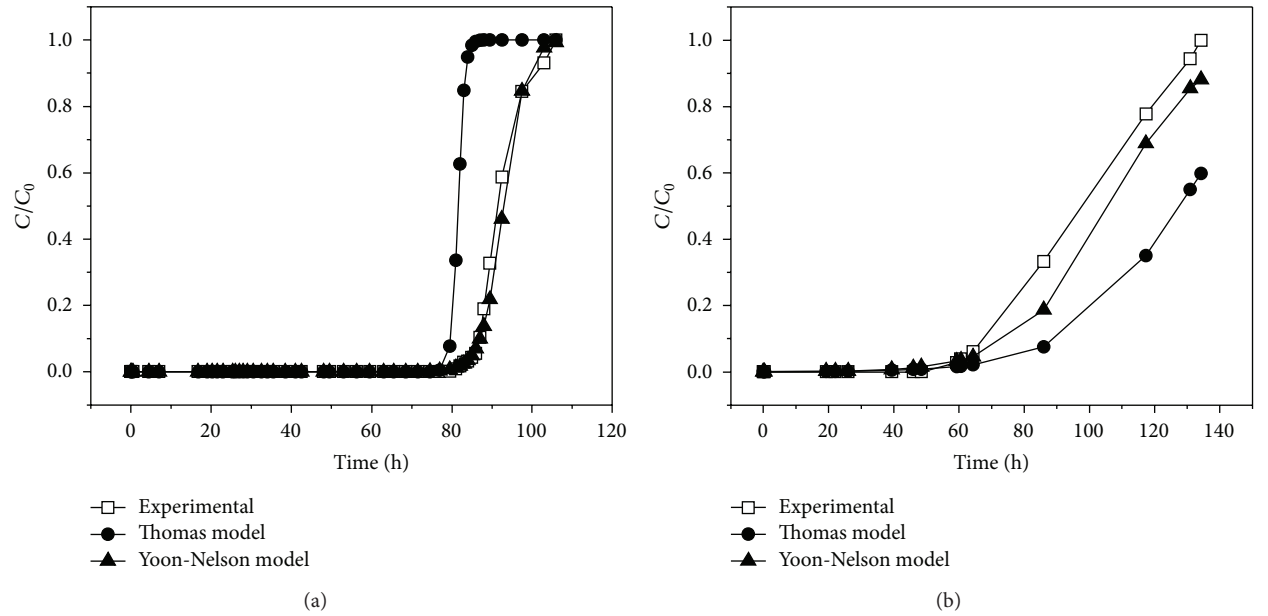

Figure 8: Predicted breakthrough curves of (a) HCl and (b) VCM on 6 N NaOH/GAC using different two models.

Table 4: Element composition of adsorbent.

Adsorbent	Na_2O	Al_2O_3	SiO_2	Cl
GAC	0.01	<0.01	0.04	0.05
6 N NaOH/GAC	5.49	<0.01	0.25	0.17
6 N NaOH/GAC adsorbed HCl-Top	0.16	<0.01	0.01	1.68
6 N NaOH/GAC adsorbed HCl-Middle	0.37	<0.01	0.01	3.89
6 N NaOH/GAC adsorbed HCl- Bottom	0.47	<0.01	0.01	4.59

be evaluated for the reaction pathways and mechanism of adsorption phenomena. The obtained parameters could be used to process upscaling. In general, two kinetic models, Thomas model and Yoon-Nelson model, are used to investigate [15]. Thomas model uses a general Langmuir isotherm and second-order reversible adsorption, while Yoon-Nelson model considers the rate of adsorption decreases relies on the proportional of adsorbate breakthrough on the adsorbents.

Thomas model can be described by (1) and is linearized for the analysis as shown in (2) [16–19]. Consider

$$\frac{C}{C_0} = \frac{1}{1 + \exp\left[K_T\left(q_0 M - C_0 V\right)/Q\right]}, \quad (1)$$

$$\ln\left(\frac{C_0}{C} - 1\right) = \frac{K_T q_0 M}{Q} - \frac{K_T C_0 V}{Q}, \quad (2)$$

where C and C_0 are the effluent and inlet gas concentration (mg/L), K_T is the Tomas rate constant (mL/min/mg), Q is volumetric flow rate (mL/min), q_0 is the maximum adsorption capacity (mg/g), M is adsorbent weight (g), and V is the throughput volume (mL). The constants, K_T and q_0, can be obtained from the intercepts and the slopes of linear plots of $\ln[(C_0/C) - 1]$ versus V. The linear plots of both HCl and VCM are presented in Figures 7(a) and 7(b).

Yoon-Nelson model can be written as the following form [20]:

$$\frac{C}{C_0} = \frac{1}{1 + \exp\left[K_{\mathrm{YN}}\left(\tau - t\right)\right]}, \quad (3)$$

where K_{YN} is Yoon-Nelson rate constant (L/min), t is sampling time (min), and τ is the time required for 50% adsorbate breakthrough (min). The linearized form of the Yoon-Nelson model is as follows:

$$\ln\left(\frac{C}{C_0 - C}\right) = K_{\mathrm{YN}} t - \tau K_{\mathrm{YN}}. \quad (4)$$

Plots of $\ln[C/(C_0 - C)]$ versus t for both HCl and VCM are shown in Figures 7(c) and 7(d). The adsorption capacity (q_0) of Yoon-Nelson model can be calculated by the following equation [21]:

$$q_0 = C_0 Q \tau. \quad (5)$$

The results of K_T, q_0, K_{YN}, and τ obtained are listed in Table 5. The theoretical predictions based on two model parameters are plotted against the experimental results in Figure 8. Normalized standard deviation (S.D.) was applied to compare the most applicable model that could describe the kinetic study of adsorption. It was obtained using the following equation [22]:

$$\text{S.D. } (\%) = 100 \times \left\{\sum \frac{\left[\left(Y_e - Y_p\right)/Y_e\right]^2}{N - 1}\right\}^{1/2}, \quad (6)$$

where Y_e is the experimental values, Y_p is the predicted values, and N is number of data points. The normalized standard deviations of the HCl and VCM adsorption on

Table 5: Calculated column kinetic parameters for HCl and VCM adsorption on 6 N NaOH/GAC.

Model	Thomas model			Yoon-Nelson model			
	K_T (mL/min/mg)	q_0 (mg/g)	S.D. (%)	K_{YN} (min^{-1})	τ (min)	q_0 (mg/g)	S.D. (%)
HCl	0.02	77.09	23.38	0.0062	5487	86.44	0.83
VCM	0.36	4.55	0.49	0.0012	6383	5.94	0.19

6 N NaOH/GAC for Thomas model are 23.38 and 0.49, respectively, while those for Yoon-Nelson model are 0.83 and 0.19, respectively, as shown in Table 5. Regarding lower normalized standard deviation, Yoon-Nelson model fit better than Thomas model.

5. Conclusions

HCl and VCM were used as probe gases for the inorganic and organic CHCs, which are poison to downstream catalysts. Several materials, including GAC, modified GAC, SiO_2, and Al_2O_3 balls, were used as adsorbents for guarding inorganic and organic CHC from H_2 feedstocks. The test was carried out in a packed column under microvolume vessel under the weight hourly space velocity range of 0.8–1.0 hr^{-1}. The adsorption capacity was analyzed by a breakthrough method. Na modified GAC showed better performance in removing HCl and VCM than other adsorbents, by chemical adsorption. In addition, the kinetic adsorption fit well with Yoon-Nelson model.

Conflict of Interests

The authors declare that there is no conflict of interests regarding the publication of this paper.

Acknowledgment

The authors would like to acknowledge PTT Public Company Limited for financial support.

References

[1] T. Kameda, N. Uchiyama, K.-S. Park, G. Grause, and T. Yoshioka, "Removal of hydrogen chloride from gaseous streams using magnesium–aluminum oxide," *Chemosphere*, vol. 73, no. 5, pp. 844–847, 2008.

[2] M. V. Twigg and M. S. Spencer, "Deactivation of copper metal catalysts for methanol decomposition, methanol steam reforming and methanol synthesis," *Topics in Catalysis*, vol. 22, no. 3-4, pp. 191–203, 2003.

[3] A. Chatterjee, T. Ebina, T. Iwasaki, and F. Mizukami, "Chlorofluorocarbons adsorption structures and energetic over faujasite type zeolites—a first principle study," *Journal of Molecular Structure: THEOCHEM*, vol. 630, no. 1–3, pp. 233–242, 2003.

[4] K. S. Walton, M. B. Abney, and M. D. LeVan, "CO_2 adsorption in y and X zeolites modified by alkali metal cation exchange," *Microporous and Mesoporous Materials*, vol. 91, no. 1–3, pp. 78–84, 2006.

[5] J. F. Scamehorn, "Removal of vinyl chloride from gaseous streams by adsorption on activated carbon," *Industrial & Engineering Chemistry Process Design and Development*, vol. 18, no. 2, pp. 210–217, 1979.

[6] H. Xiao, H. Peng, S. Deng, X. Yang, Y. Zhang, and Y. Li, "Preparation of activated carbon from edible fungi residue by microwave assisted K_2CO_3 activation—application in reactive black 5 adsorption from aqueous solution," *Bioresource Technology*, vol. 111, pp. 127–133, 2012.

[7] F. Rodríguez-Reinoso and M. Molina-Sabio, "Textural and chemical characterization of microporous carbons," *Advances in Colloid and Interface Science*, vol. 76-77, pp. 271–294, 1998.

[8] M.-T. Lee, Z.-Q. Wang, and J.-R. Chang, "Activated-carbon-supported NaOH for removal of HCl from reformer process streams," *Industrial and Engineering Chemistry Research*, vol. 42, no. 24, pp. 6166–6170, 2003.

[9] B.-J. Kim, H. Park, and S.-J. Park, "Toxic gas removal behaviors of porous carbons in the presence of Ag/Ni bimetallic clusters," *Bulletin of the Korean Chemical Society*, vol. 29, no. 4, pp. 782–784, 2008.

[10] S.-J. Park and S.-Y. Jin, "HCl removal using activated carbon fibers electroplated with silver," *Carbon*, vol. 42, no. 10, pp. 2113–2115, 2004.

[11] S.-J. Park and S.-Y. Jin, "Effect of nickel electroplating on HCl removal efficiency of activated carbon fibers," *Journal of Industrial and Engineering Chemistry*, vol. 11, no. 3, pp. 395–399, 2005.

[12] K. Oksman, A. P. Mathew, D. Bondeson, and I. Kvien, "Manufacturing process of cellulose whiskers/polylactic acid nanocomposites," *Composites Science and Technology*, vol. 66, no. 15, pp. 2776–2784, 2006.

[13] A. Gani and I. Naruse, "Effect of cellulose and lignin content on pyrolysis and combustion characteristics for several types of biomass," *Renewable Energy*, vol. 32, no. 4, pp. 649–661, 2007.

[14] C. Bouchelta, M. S. Medjram, O. Bertrand, and J.-P. Bellat, "Preparation and characterization of activated carbon from date stones by physical activation with steam," *Journal of Analytical and Applied Pyrolysis*, vol. 82, no. 1, pp. 70–77, 2008.

[15] J. T. Nwabanne and P. K. Igbokwe, "Kinetic modeling of heavy metals adsorption on fixed bed column," *International Journal of Environmental Research*, vol. 6, no. 4, pp. 945–952, 2012.

[16] T. Mathialagan and T. Viraraghavan, "Adsorption of cadmium from aqueous solutions by perlite," *Journal of Hazardous Materials*, vol. 94, no. 3, pp. 291–303, 2002.

[17] W. Zou, L. Zhao, and R. Han, "Removal of Uranium (VI) by fixed bed ion-exchange column using natural zeolite coated with manganese oxide," *Chinese Journal of Chemical Engineering*, vol. 17, no. 4, pp. 585–593, 2009.

[18] A. B. Albadarin, C. Mangwandi, A. H. Al-Muhtaseb, G. M. Walker, S. J. Allen, and M. N. M. Ahmad, "Modelling and fixed bed column adsorption of Cr(VI) onto orthophosphoric acid-activated lignin," *Chinese Journal of Chemical Engineering*, vol. 20, no. 3, pp. 469–477, 2012.

[19] C. Xiong, Y. Li, G. Wang et al., "Selective removal of Hg(II) with polyacrylonitrile-2-amino-1,3,4-thiadiazole chelating resin: batch and column study," *Chemical Engineering Journal*, vol. 259, pp. 257–265, 2015.

[20] Z. Aksu and F. Gönen, "Biosorption of phenol by immobilized activated sludge in a continuous packed bed: prediction of breakthrough curves," *Process Biochemistry*, vol. 39, no. 5, pp. 599–613, 2004.

[21] S. H. Lin and C. S. Wang, "Treatment of high-strength phenolic wastewater by a new two-step method," *Journal of Hazardous Materials*, vol. 90, no. 2, pp. 205–216, 2002.

[22] B. H. Hameed, A. A. Ahmad, and N. Aziz, "Isotherms, kinetics and thermodynamics of acid dye adsorption on activated palm ash," *Chemical Engineering Journal*, vol. 133, no. 1–3, pp. 195–203, 2007.